

Supplemental Material

Supplemental Methods – Algorithm Description

The underlying concept of the LVO detection presented here relies on software that is able to detect reduced opacification and number of anterior intracranial vessels. It is composed of eight major steps (**Fig. 1** of main manuscript):

1. *Data Import:* Native, thin-slice CTA DICOM images are imported into the software.
2. *Pre-Processing:* **a.** Trim CTA input data to keep only slices located between C1 vertebrae and vertex. **b.** Remove CT head holder from all CTA images.
3. *Identify Anatomy:* **a.** An anatomic template of a human head is elastically aligned with the patient's CTA dataset using non-rigid registration¹. **b.** Templates of relevant anatomic structures (e.g. bones, vessels) and the three pre-specified hemispheric regions of interest (R1, R2, and R3) relevant for subsequent analysis (defined in the coordinate space of the anatomic template) are warped onto the patient's CTA using the transformation parameters determined in **(a)**. Of note here, the R2 region covers the M2-MCA segment from its genu half-way to the top of the Sylvian cistern.
4. *Bone Removal:* Using the bone mask defined in step 2, the skull base and calvarium are removed from the CTA volume.
5. *Vessel Detection:* Intracranial vessels are identified and categorized into large and small diameter vessel groups using *tubular filtering*².
6. *Evaluate Regions:* **a.** The total sum of voxel densities (in Hounsfield Units) within the large caliber vessels – the intracranial ICA and proximal M1-MCA segment (R1 in **Fig. 1**) – is assessed together with each vessel's segment length. **b.** For “small caliber” vessels – the mid-to-distal M1 (R2), M2, and more distal MCA segments (R3) – the total sum of voxel densities (as determined in the previous step) is measured.
7. *Abnormality Detection:* **a.** Density metrics for R1, R2, and R3 are compared between hemispheres. **b.** The following thresholds for relative hemispheric vessel density ratio and corresponding color schemes were used: <80%-75% (BLUE); <75%-60% (GREEN); <60%-45% (YELLOW); and <45% (RED). Here, the percentage indicates the fraction of signal relative to the opposite hemisphere, i.e. <45% (RED) constitutes the greatest drop in vessel density whereas <80%-75% is the most mild reduction. **c.** The regions are priority ranked from R1 to R3 with R1 given the highest priority. That is, the algorithm compares R1 regions in both hemispheres first and only progresses to the next regions (i.e. R2 and then R3) if the density reduction did not meet the chosen severity threshold.
8. *Report Generation:* **a.** De-tilted and rotation-corrected axial, coronal, and sagittal *maximum intensity projections* (MIPs) of the intracranial vasculature were rendered from the bone-masked CTA volumes. **b.** The regions R1, R2, or R3 – depending on which are deemed abnormal (based on the aforementioned metrics) – are highlighted as color overlays on the MIP images. For simplicity of review, only the most proximal region demonstrating hemispheric abnormality is shown on the overlay. **c.** Annotated and unannotated MIPs are then exported as secondary capture DICOM images.

Supplemental References

1. Klein S, Staring M, Murphy K, Viergever MA. Elastix: A toolbox for intensity based medical image registration. *IEEE Transactions on Medical Imaging*. 2010;29:196-205
2. Frangi AF, Niessen WJ, Vincken KL, Viergever MA. Multiscale vessel enhancement filtering. *Medical image computing and computer-assisted intervention - miccai'98*. 1998;1496:130-137

Supplemental Figures

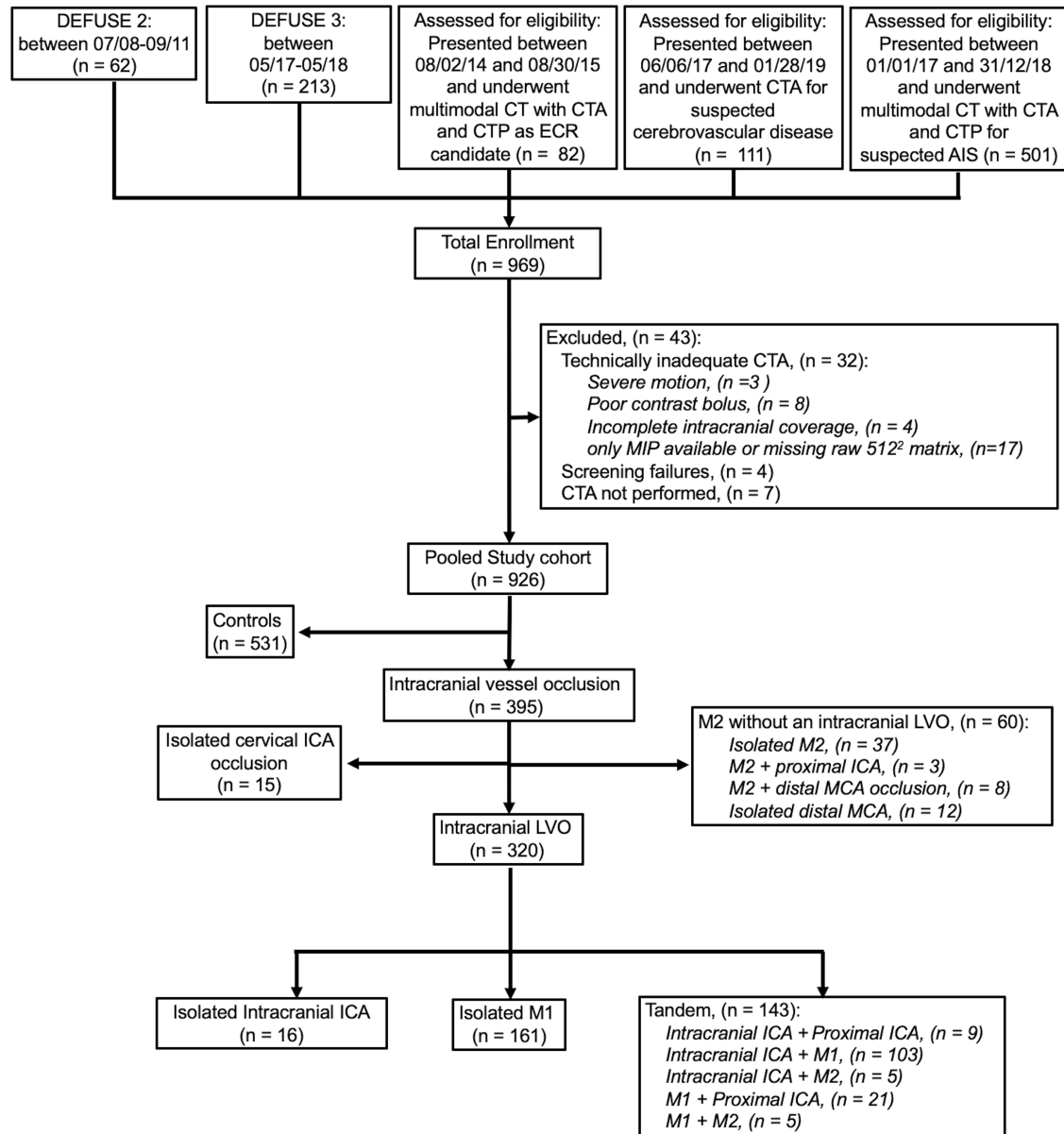


Figure I – Cohort selection flow chart.

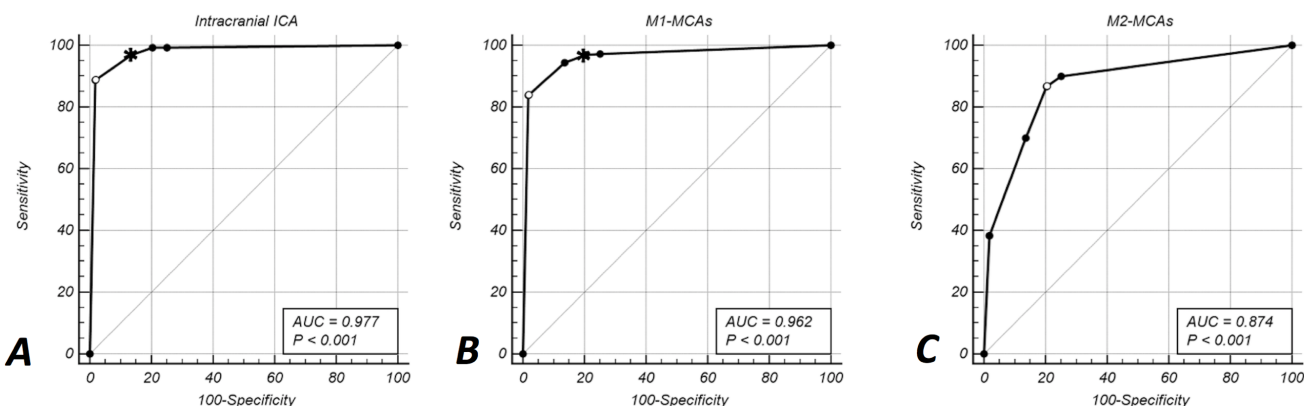


Figure II – ROC Analysis for occlusion of individual vessel segments. Diagnostic performance for detection of intracranial ICA occlusions (**A**) was almost perfect, with excellent performance also for M1-MCA occlusions (**B**) and good performance for M2-MCA occlusions (**C**). Dots on the ROC curve indicate individual threshold levels; the one with the lowest sensitivity and highest specificity is the <45% threshold whereas the highest sensitivity and lowest specificity were at the <80%-75% threshold. The open circle indicates the maximum Youden index. The asterisks indicate the threshold at which the ≥95% sensitivity target was reached with the highest specificity. The significance level in the legend indicates the p-value of the z-statistic derived from the DeLong algorithm

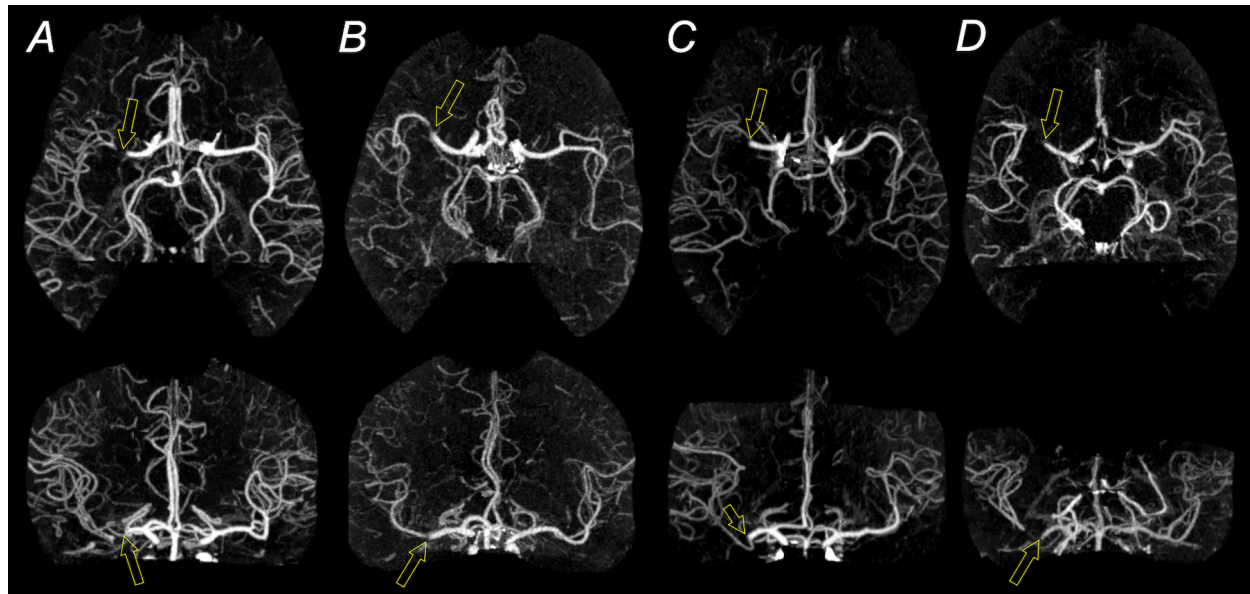


Figure III – False Negative Results. (A)-(B) show axial and coronal MIPs of patients with short-segment M1-MCA occlusions (open arrows) with good collaterals reconstituting the distal M1 segment and the M2 segments, indicated by high luminal density (“CTA signal”) distal to the occlusion, albeit with reduced caliber. (A) 76-yo female with a right mid M1 occlusion. (B) 61-yo male with a right distal M1 occlusion. (C)-(D) show two patients with complete mid-M1 occlusions (open arrows). Both patients had robust collaterals, indicated by opacification of the proximal M2 segments, that led to the negative output of the algorithm.

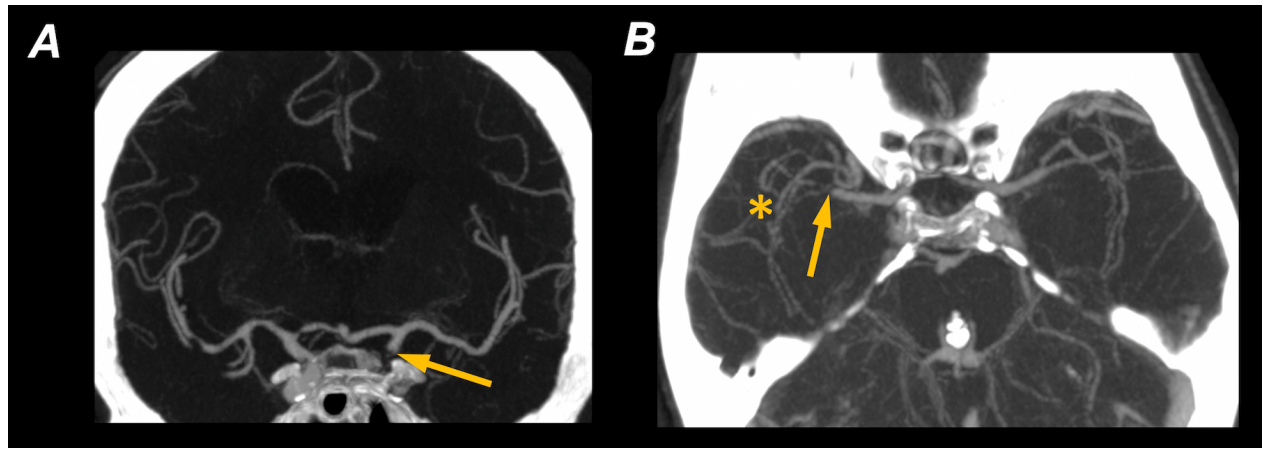


Figure IV – False negative examples at softest (BLUE) threshold. (A) Skull base ICA occlusion (arrow). Opacification of the supraclinoid ICA and distal to region highlighted by the yellow arrow led to a false negative detection. (B) One out of five false negatives with mid-to-distal M1 occlusion (arrow) with prominent collaterals (asterisk) immediately distal to occlusion.

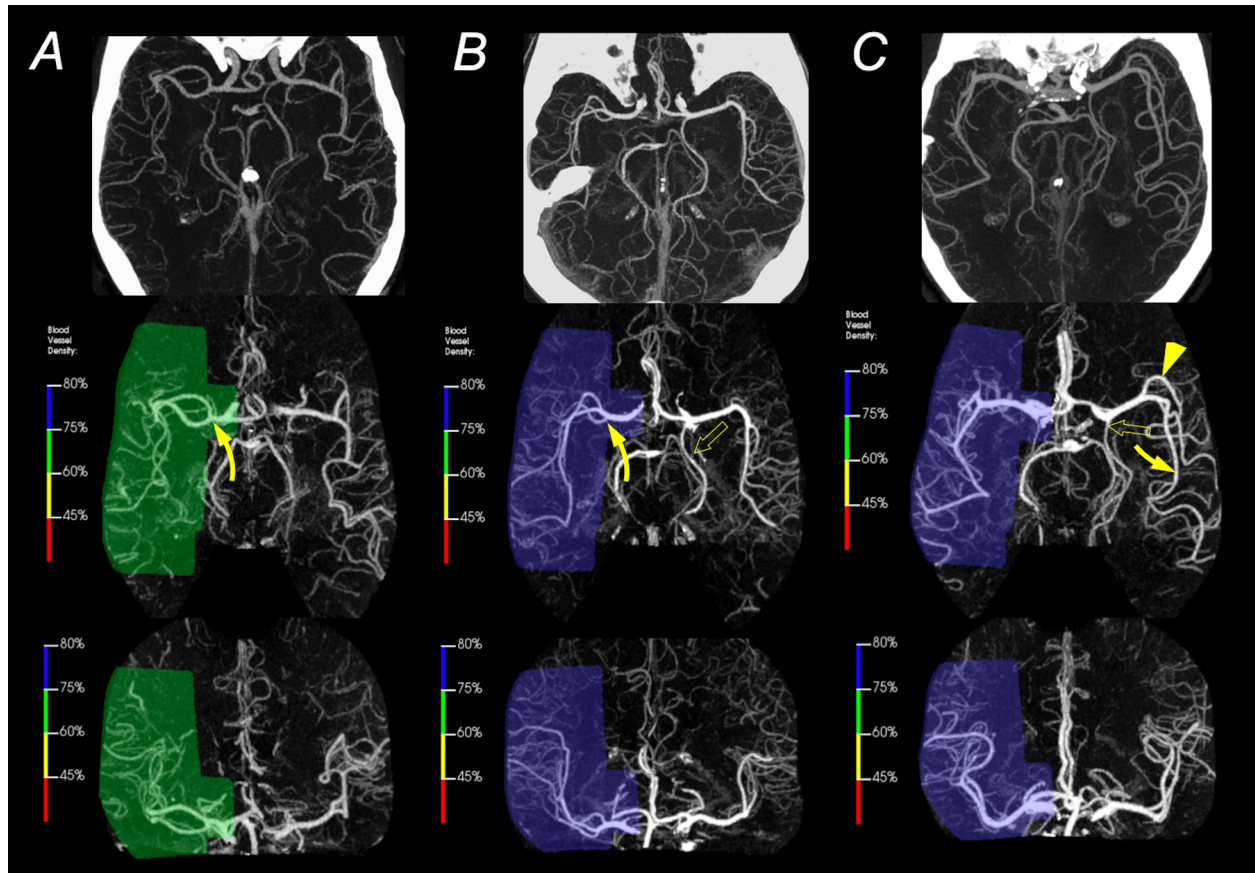


Figure V – False Positive Results related to Normal Variants. (A) 67-yo male with a very early bifurcation of the right M1-MCA (curved arrow) and consequently more prominent distal vessels in the left hemisphere. (B) 68-yo male with an early trifurcation of the right M1-MCA (curved arrow) resulting in greater prominence of the left MCA M1 segment and distal branches. A left fetal PCA (open arrow) was also present and contributed to the hemispheric asymmetry in vessel density. (C) 71-yo male with prominent anterior (arrowhead) and posterior (curved arrow) M2 divisions relative to their contralateral counterparts. A left fetal PCA (open arrow) contributed to further hemispheric imbalance. Corresponding original thin slice MIPs (top row) are added as color overlays exaggerate vessel density which makes it harder to appreciate the reduced vessel density.

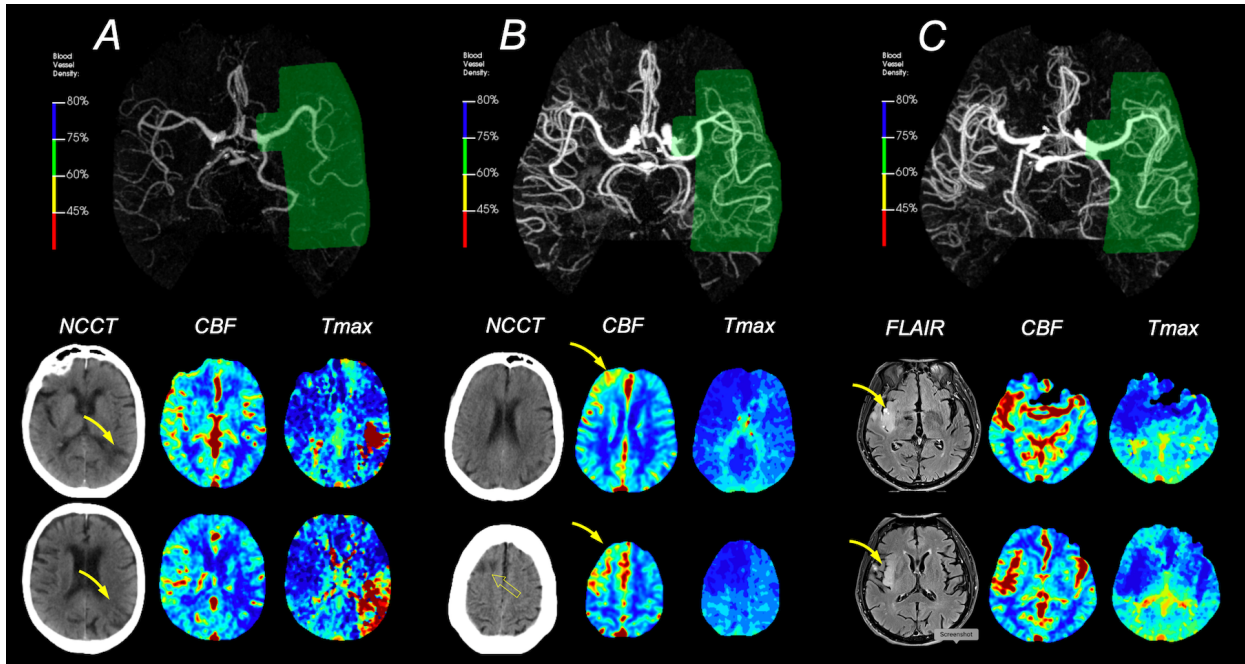


Figure VI – False Positive Results from other pathology. (A) 89-yo male with an old infarct (curved arrow) within the posterior aspect of the left MCA territory (distal inferior M2 subdivision). Reduced blood flow and high Tmax from CTP is also shown. There was a chronic occlusion of the distal inferior M2 division, resulting in a paucity of vessels in the infarcted region and hemispheric imbalance (green region). (B) 82-yo female with hyperperfusion in the right anterior MCA and ACA territory (curved arrow) and hypodensity on NCCT (open arrow). likely due to a reperfused acute infarct. The substantially higher flow within this area (seen best on perfusion parametric maps as elevated relative CBF and decreased Tmax) increased the overall vessel density, which in turn led to asymmetry which was interpreted by the algorithm as lower CTA opacification in the contralateral hemisphere. (C) 79-yo male patient with a GBM in the right insula (curved arrow). Hypervascularity related to the tumor itself and and seizure activity led to increased blood flow (best appreciated on CBF and Tmax maps) within and adjacent to the insula, which increased overall CTA opacification in this region relative to the contralateral hemisphere.

Supplemental Tables

The five tables below provide the full confusion matrices for all tests performed and will allow interested researchers to reproduce the ROC analyses performed for this study.

Table Ia – Diagnostic Performance for LVOs

threshold	0	1	2	3
TP	311	310	300	264
FP (type 1)	180	151	106	28
TN	408	437	482	560
FN (type 2)	9	10	20	56
1-Spec	30.61%	25.68%	18.03%	4.76%
Sens	97.19%	96.88%	93.75%	82.50%
Spec	69.39%	74.32%	81.97%	95.24%
PPV	63.34%	67.25%	73.89%	90.41%
NPV	97.84%	97.76%	96.02%	90.91%
Accuracy	79.19%	82.27%	86.12%	90.75%
Youden J	0.6658	0.7119	0.7572	0.7774

threshold that meets $\geq 95\%$ sensitivity requirement at highest achievable specificity

threshold that yields the maximum Youden index, J_{max}

Table Ib – Diagnostic Performance for LVOs, incl. M2-MCAs

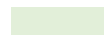
threshold	0	1	2	3
TP	354	351	334	282
FP (type 1)	139	112	74	11
TN	404	431	469	532
FN (type 2)	14	17	34	86
1-Spec	25.60%	20.63%	13.63%	2.03%
Sens	96.20%	95.38%	90.76%	76.63%
Spec	74.40%	79.37%	86.37%	97.97%
PPV	71.81%	75.81%	81.86%	96.25%
NPV	96.65%	96.21%	93.24%	86.08%
Accuracy	83.21%	85.84%	88.14%	89.35%
Youden J	0.7060	0.7475	0.7713	0.7460

threshold that meets $\geq 95\%$ sensitivity requirement at highest achievable specificity

threshold that yields the maximum Youden index, J_{max}

Table IIa – Diagnostic Performance for Intracranial ICAs alone

threshold	0	1	2	3
TP	132	132	129	118
FP	133	108	72	10
TN	398	423	459	521
FN	1	1	4	15
1-Spec	25.05%	20.34%	13.56%	1.88%
Sens	99.25%	99.25%	96.99%	88.72%
Spec	74.95%	79.66%	86.44%	98.12%
PPV	49.81%	55.00%	64.18%	92.19%
NPV	99.75%	99.76%	99.14%	97.20%
Accuracy	79.82%	83.58%	88.55%	96.23%
Youden J	0.7420	0.7891	0.8343	0.8684

 threshold that meets $\geq 95\%$ sensitivity requirement at highest achievable specificity

 threshold that yields the maximum Youden index, J_{max}

Table IIb – Diagnostic Performance for M1 - MCAs alone

threshold	0	1	2	3
TP	282	281	274	243
FP	133	108	72	10
TN	398	423	459	521
FN	8	9	16	47
1-Spec	25.05%	20.34%	13.56%	1.88%
Sens	97.24%	96.90%	94.48%	83.79%
Spec	74.95%	79.66%	86.44%	98.12%
PPV	67.95%	72.24%	79.19%	96.05%
NPV	98.03%	97.92%	96.63%	91.73%
Accuracy	82.83%	85.75%	89.28%	93.06%
Youden J	0.7219	0.7656	0.8092	0.8191

 threshold that meets $\geq 95\%$ sensitivity requirement at highest achievable specificity

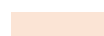
 threshold that yields the maximum Youden index, J_{max}

Table IIc – Diagnostic Performance for M2 - MCAs alone

threshold	0	1	2	3
TP	54	52	42	23
FP	133	108	72	10
TN	398	423	459	521
FN	6	8	18	37
1-Spec	25.05%	20.34%	13.56%	1.88%
Sens	90.00%	86.67%	70.00%	38.33%
Spec	74.95%	79.66%	86.44%	98.12%
PPV	28.88%	32.50%	36.84%	69.70%
NPV	98.51%	98.14%	96.23%	93.37%
Accuracy	76.48%	80.37%	84.77%	92.05%
Youden J	0.6495	0.6633	0.5644	0.3645

 threshold that meets $\geq 95\%$ sensitivity requirement at highest achievable specificity

 threshold that yields the maximum Youden index, J_{max}